Thieme

Modern Cartilage Imaging of the Ankle

Moderne Knorpelbildgebung des Sprunggelenks

Authors
Marc-André Weber[1], Felix Wünnemann[1], Pia M. Jungmann[2], Benita Kuni[3], Christoph Rehnitz[1]

Affiliations
1 University Hospital Heidelberg, Diagnostic and Interventional Radiology, Heidelberg, Germany
2 Radiology, Technical University of Munich, Germany
3 Orthopedics and Trauma Surgery, Ortho-Zentrum Karlsruhe, Germany

Key words
ankle, cartilage, MR-imaging, osteochondral lesions, treatment effects, trauma

received 23.11.2016
accepted 08.04.2017

Bibliography
DOI https://doi.org/10.1055/s-0043-110861
Published online: 11.7.2017 | Fortschr Röntgenstr 2017; 189: 945–956 © Georg Thieme Verlag KG, Stuttgart · New York, ISSN 1438-9029

Correspondence
Prof. Marc-André Weber
Universitätsklinik Heidelberg, Diagnostische und Interventionelle Radiologie, Im Neuenheimer Feld 110, D-69120 Heidelberg, Germany
Tel.: ++ 49/62 21/56 74 20
Fax: ++ 49/62 21/56 54 20
MarcAndre.Weber@med.uni-heidelberg.de

ABSTRACT

Background Talar osteochondral lesions are an important risk factor for the development of talar osteoarthritis. Furthermore, osteochondral lesions might explain persistent ankle pain. Early diagnosis of accompanying chondral defects is important to establish the optimal therapy strategy and thereby delaying or preventing the onset of osteoarthritis. The purpose of this review is to explain modern cartilage imaging with emphasis of MR imaging as well as the discussion of more sophisticated imaging studies like CT-arthrography or functional MR imaging.

Methods Pubmed literature search concerning: osteochondral lesions, cartilage damage, ankle joint, talus, 2 D MR imaging, 3 D MR imaging, cartilage MR imaging, CT-arthrography, cartilage repair, microfracture, OATS, MACT.

Results and Conclusion Dedicated MR imaging protocols to delineate talar cartilage and the appearance of acute and chronic osteochondral lesions were discussed. Recent developments of MR imaging, such as isotropic 3 D imaging that has a higher signal-to noise ratio when compared to 2 D imaging, and specialized imaging methods such as CT-arthrography as well as functional MR imaging were introduced. Several classifications schemes and imaging findings of osteochondral lesions that influence the conservative or surgical therapy strategy were discussed. MRI enables after surgery the non-invasive assessment of the repair tissue and the success of implantation.

Key points

- Modern MRI allows for highly resolved visualization of the articular cartilage of the ankle joint and of subchondral pathologies.
- Recent advances in MRI include 3 D isotropic ankle joint imaging, which deliver higher signal-to-noise ratios of the cartilage and less partial volume artifacts when compared with standard 2 D sequences.
- In case of osteochondral lesions MRI is beneficial for assessing the stability of the osteochondral fragment and for this discontinuity of the cartilage layer is an important factor.
- CT-arthrography can be used in case of contraindications of MRI and in unclear MRI findings as further diagnostic approach.

Citation Format

- Weber MA, Wünnemann F, Jungmann PM et al. Modern Cartilage Imaging of the Ankle. Fortschr Röntgenstr 2017; 189: 945–956

ZUSAMMENFASSUNG

Hintergrund Osteochondrale Läsionen am Talus sind ein wichtiger Risikofaktor bei der Entstehung einer Arthrose am Sprunggelenk. Zudem können osteochondrale Läsionen eine Erklärung für persistierende Sprunggelenkbeschwerden sein. Eine frühzeitige Erkennung von Knorpelschäden und Begleiterscheinungen ist wichtig, um das optimale Therapieregime zu etablieren und so die Entstehung einer Arthrose zu verzögern oder sogar zur verhindern. Ziel dieser Übersichtsarbeit ist die Erläuterung der modernen Knorpelbildung mit Betonung der MRT und Diskussion von Spezialuntersuchungen wie der CT-Arthrographie sowie der funktionellen MR-Bildgebung.

Methode Pubmed Literaturrecherche zu den Stichworten: osteochondral lesions, cartilage damage, ankle joint, talus,

2 D MR imaging, 3 D MR imaging, cartilage MR imaging, CT-arthrography, cartilage repair, microfracture, OATS, MACT.

Ergebnisse und Schlussfolgerungen Dezidierte MR-Protokolle zur Abgrenzung des Gelenkknorpels sowie das Erscheinungsbild aktuer und chronischer osteochondraler Läsionen werden diskutiert. Neue Entwicklungen der MRT wie die dreidimensionale (3 D)-Isotrope Sprunggelenkbildgebung, die ein höheres Signal-Rausch-Verhältnis des Knorpels im Vergleich zu zweidimensionalen Sequenzen aufweist, sowie Spezialuntersuchungen wie die CT-Arthrographie und die funktionelle MR-Bildgebung werden vorgestellt. Verschiedene Klassifikationssysteme und bildgebende Befunde von osteochondralen Läsionen, die eine Entscheidung zur konservativen oder operativen Therapie beeinflussen, werden erläutert. Die MRT ermöglicht postoperativ die nicht-invasive Beurteilung der Knorpelregeneratbildung und den Erfolg der Implantation.

Introduction

Why is dedicated ankle cartilage imaging important? During a normal walking sequence, forces of up to five times the body weight [1] act on ankle cartilage which, as these forces increase, raise the risk of osteoarthritis [2], thus emphasizing the importance of cartilage as a buffer zone as well as the clinical relevance of cartilage damage. Indications for dedicated cartilage imaging therefore include identification of osteochondral lesions with regard to their size, composition and stability. Verification of such cartilage-bone defects requires imaging in two planes. Early detection is important, since post-traumatic cartilage damage and osteochondral lesions of the talus can cause persistent anomalies in the ankle, and ultimately result in post-traumatic osteoarthritis [3]. Furthermore, in addition to lesion detection, preoperative classification into stable and unstable osteochondral lesions is crucial. Postoperative follow-up assessment after cartilage therapy is also an important indication for dedicated cartilage imaging at the ankle joint. MRI is the most common imaging modality for planning of cartilage replacement therapy for osteochondral lesions [4], since MRI is particularly suitable for the evaluation of deep chondral delaminations and subchondral lesions which are not detectable arthroscopically if the superficial cartilage layer is intact. Along with the accurate assessment of the cartilage layer and detection of possible delaminations, the condition of the subchondral bone has an influence on operative therapy decisions regarding ante- or retrograde drilling or (osteo-) chondral transplantation procedures [5, 6]. CT arthrography often proves to be a useful supplement in the case of unclear MRI findings with respect to cartilage delamination. Further indications for MRI include suspected post-traumatic cartilage damage in unremarkable radiographs or CT or the assessment of the cartilage when an osteophyte is detected with regard to the question whether an arthroscopic osteophyte ablation or arthrodesis is called for [7]. On the other hand, imaging of the very thin ankle cartilage with an average 1.1 mm (0.4 – 2.1 mm) thickness is a challenge for imaging [8]. Even with optimized 2 D sequence protocols, identification of defects other than the entire cartilage layer as well as fissures is a further challenge. Fortunately, however, defects that do not affect the entire cartilage layer are generally treated conservatively.

Imaging Modalities

Projection radiography

Conventional projection radiography in two planes is the first step toward to the diagnosis of an acute osteochondral injury using minimal imaging of a fresh injury to the upper ankle [9]. A “clicking” feeling and blockage in the upper ankle are indications of a dislocated fragment. On the one hand, the subchondral fracture may already be visible on the radiograph, and on the other hand, a detached fragment can be detected (▶ **Fig. 1a, b**). The distinction between acute and chronic osteochondral lesions is difficult using X-ray and is often only possible taking into account the mechanism and time of the incident. An MRI is indispensable for more extensive diagnosis [9, 10].

Magnetic resonance imaging and sequence protocol

Current MRI technology allows the cartilage of the upper ankle to be displayed in high resolution. At 3 Tesla even routine (2 D) sequences with an in-plane resolution of less than 0.5 mm can be acquired. Recently available three-dimensional (3 D) sequences also promise further improvement in resolution. On the other hand, an intervening fluid lamella often makes it impossible to distinguish between the tibial and talar cartilage surfaces using modern sequence techniques (▶ **Fig. 1c**). In this case, distension of the upper ankle using traction technique can lead to an increase in the differentiability. Due the small thickness of the cartilage layer, partial volume effects, particularly in the edge region, are possible. According to studies, the sensitivity of the cartilage lesion image varies from 50 % at 1.5 Tesla and 75 % at 3 Tesla field strength [10]; improvements in diagnostic power can be expected as the technology is developed further. In the clinical setting of most institutions, a routine ankle protocol is used that requires high-resolution sequences suitable for the assessment of articular cartilage. For the examination of the ankle, the patient is placed in a supine position with the ankle in a neutral position, i. e. with a right angle between the foot and lower leg. Different positions such as the prone position with maximum plantar flexion of the foot [11] and the supine position with 20 degrees plantar flexion [12] are also possible and have been suggested by other authors. The prone position with maximum plantar flexion of the foot offers the advantages of good fixation possibility and results in fewer movement artifacts and absent magic angle artifacts in the course of the tendons around the ankle [11]. In

▶ **Fig. 1 a, b** 25-year-old dance sportswoman with chronic pain at the right medial malleolus. The a.-p. projection radiography **a** shows by means of increase in transparency and structural irregularities an osteochondral lesion if the medial talar dome (arrow). The coronal proton density (PD) weighted fat suppressed sequence **b** demonstrates fluid in between the fragment and the adjacent bone (arrows), but no dislocation of the fragment (stage III according to Nelson and Dipaola). **c** The sagittal 3 D T2*-weighted MEDIC 3 Tesla sequence without the use of axial traction illustrates the thin cartilage layer of the talar dome (arrow) and the missing separation between the cartilage surfaces of the tibial plafond and talar dome in this 16-year-old adolescent who suffered from ankle sprain and sprain of the deltoid ligament. **d–f** 2 D sequences recommended 2006 by the German Radiological Society [13] for depicting osteochondral lesions of the ankle, **d** coronal PD-weighted fat suppressed sequence, **e** coronal T1-weighting, **f** sagittal PD-weighting; additionally, an axial T2-weighting is recommended (not shown).

our opinion, however, comfortable patient positioning and high-resolution imaging are ideally achieved using dedicated multichannel coils. In our facility we utilize a 4-channel flex coil (366 × 174 mm); the following protocol was developed on a clinical 3-Tesla system (▶ **Table 1**). The manufacturers also offer dedicated ankle coils. A small image field of 12 – 16 cm and slice thicknesses of max. 3 mm in three spatial directions are important [13]. In particular proton density (PD) or intermediate-weighted, fat suppressed sequences are used in the sagittal, axial and coronal slice planes. These sequences are supplemented by a coronal T1-weighted sequence and a sagittally planned 3 D sequence with isotropic voxel size in the submillimeter range (▶ **Fig. 1**). We do not recommend routine intravenous contrast to assess post-traumatic cartilage damage. When planning the coronal slices, the ankle mortise serves as a reference, sagittal planning takes place perpendicular to the coronal, and the axial layers are transversally planned through the ankle.

Current three-dimensional sequences promise a further gain in spatial resolution and secondary reconstruction possibilities in any spatial direction. For example, a T2- or PD-weighted, fat-suppressed SPACE sequence (Sampling Perfection with Application Optimized Contrast with Different Flip Angle Evolution) or a T2*-weighted MEDIC (Multi-Echo Data Image Combination) sequence are suitable for cartilage imaging. 3 D techniques have the advantage of isotropic voxels without a gap between the individual layers (▶ **Fig. 2**). They reduce partial volume effects (mainly due to the curved cartilage surface of the talus) and according to current studies, have a higher contrast-to-noise ratio [14] or signal-to-noise ratio [15] in the cartilage compared to fluid. In one of these studies, a higher diagnostic confidence of two investigators was established, and more cartilage defects were found compared to two-dimensional sequences [14]. In contrast, a recent arthroscopically-controlled study [16] found no significant difference in the detection of talar cartilage lesions. It has not yet be finally clarified whether the theoretical advantage of the higher resolution of 3 D sequences is reflected in an actual diagnostic gain. In practice, these sequences can be recommended as a supplement, especially in difficult or unclear cases.

A further technical possibility is axial traction which can improve the separation of the cartilage layers and thus also enhance lesion detection. Using axial tensile forces (for example, 6 kg) in asymptomatic ankle joints, an enlargement of the joint gap could be achieved without intra-articular contrast medium application, thus providing improved visualization of the cartilage surface [17]. There were no increased movement artifacts, and no subject terminated the examination. In the study of axial traction, the T1-weighted sequence was best evaluated with a driven equilibrium pulse (DRIVE) [17]. As shown in the examples, in the case of the T1-weighted DRIVE sequence, signal-rich joint fluid with a good demarcation of the cartilage surface is obtained with otherwise normal T1 contrast [18] (▶ **Fig. 3**)

Additional technologies: MR and CT arthrography

As a rule, after the clinical examination, conventional X-ray diagnostics in orthopedics is the primary imaging modality for ankle joint problems [19]. In the case of unexplained discomfort in the upper ankle, such as persistent post-traumatic complaints without evidence of fracture, native MR imaging is usually carried out, in particular with respect to the presence of an osteochondral lesion (OCL) or a ligament injury. CT arthrography is a very good method to detect cartilage defects on the upper ankle (▶ **Fig. 4**) [20]. It can be used when MRI is contraindicated as well as for advanced diagnosis in the case of unclear MRI findings in the assessment of the integrity of articular cartilage or for further clarification of detected chondral or osteochondral lesions, in particular if the findings influence the therapy decision [20]. Compared to 1.5 and 1 Tesla MR arthrography, CT arthrography showed an even higher agreement among 3 evaluators and

▶ **Table 1** 3 Tesla MRI protocol used in house for depiction of cartilage- and trauma-related issues of the ankle joint.

no.	sequence	TR (ms)	TE (ms)	voxels (mm^3)	TA (min)
1	localizer (gradient echo)	13	4.92	0.6 × 0.6 × 6.0	0:37
2	3 D Scout ankle	3.4	1.26	1.7 × 1.7 × 1.7	0:27
3	coronal PDw TSE fatsat (pat 2)	3230	26	0.4 × 0.4 × 2.5	2:43
4	sagittal PDw TSE fatsat (pat 2)	3110	25	0.4 × 0.4 × 2.5	3:17
5	axial PDw TSE fatsat (pat 2)	2880	23	0.4 × 0.4 × 2.5	4:03
6	coronal T1w	750	14	0.4 × 0.4 × 2.5	3:38
7	sagittal T2*w 3 D MEDIC (pat 2)	41	22	0.6 × 0.6 × 0.6	5:37
	optional				
8	axial T2w TSE (pat 2)	3260	95	0.5 × 0.5 × 3.0	4:19
9	sagittal STIR (pat 2)	5870	44	0.6 × 0.5 × 2.5	4:02
10	sagital T2w TSE (pat 2)	2660	95	0.6 × 0.4 × 2.5	2:44

TSE = turbo spin echo, 3 D = three-dimensional, PD = proton density, w = weighted, fatsat = with fat suppression, STIR = short tau inversion recovery, MEDIC = Multi-Echo Data Image Combination, pat 2 = parallel acquisition technique with an acceleration factor of 2.

provided a higher degree of reliability in cartilage lesions in this now 13-year-old study [7]. To date there are no prospective comparisons of CT arthrography versus 3 Tesla MRI. Disadvantages of CT arthrography are radiation exposure and higher invasivity compared to native MRI (possibly with traction). In most centers in Germany, routine application of direct MR arthrography [21] has not been established in the diagnosis of cartilage-related issues of the ankle. In borderline cases both techniques can supplement a native MRI, for example when determining the stability of osteochondral lesions. Especially with respect to the integrity of the cartilage layer and the stability of a known OCL, MR or CT arthrography can provide important additional information that can demonstrate instability of the OCL by contrast agent injection into the cartilage and around the fragment (partially or completely in the case of detachment) [22]. In addition, the possible fissural contact of an intraosseous ganglion can be demonstrated after intra-articular injection [20]. These special examinations are particularly suitable if important therapeutic decisions and prognostic assessments depend on the findings, as is the case in our cohort for instance in high-performance athletes.

Intra-articular contrast medium injection for CT and MR arthrography is performed under fluoroscopy control and sterile conditions by means of anterior or medial access while avoiding the dorsalis pedis artery by means of a 20 – 22 gauge needle [7, 23]. For the arthrography, a test infusion of local anesthetic (e. g., lidocaine 2 %) as well as iodine-based contrast agent is used to confirm the intra-articular needle position. Subsequently, 6 – 8 ml iodine-based contrast agent (200 mg / ml) is injected for CT arthrography and 6 – 8 ml gadolinium-based contrast agent (2 mmol / l) is used for the MR arthrography. Prompt performance of tomography is important in order to avoid the resorption of the contrast agent as well as the diffusion of the contrast medium into the articular cartilage while precluding false defects [24]. CT acquisition generally uses a tube voltage of 120 kVp and a current-time-product of 100 mAs. Reconstructions are performed in all three planes using a U70v kernel and a layer thickness of 2 mm in the bone window. Fissural defects may sometimes be overlooked at this slice thickness but which can be detected using 1 mm reconstructions.

Focal cartilage damage of the ankle

Acute cartilage damage on the ankle joint usually affects the joint surface of the talus and runs parallel to the cartilage surface, and is limited to the cartilage and/or the directly subchondral bone. Subchondral trabecular micro-fractures (bone bruises), osteochondral fractures and fractures limited to articular cartilage are, according to current doctrine, different manifestations of impact injuries to the joint surface [9, 25]. Critical to the description of the cartilage lesion are localization and size, its depth and limitation, accompanying bone marrow edema, which are often associated with pain, as well as any subchondral cysts. Measurement of the bony fragment and subchondral cysts is important for therapy planning, since size has an influence on the therapy chosen [26]. Large cysts or defects can be filled with bone material, for example. It is also important to note whether the cartilaginous lesion is located in the anterior two-thirds of the joint, since anterior access is necessary for arthroscopically guided therapy. If, however, the lesion is located in the posterior third of the joint, posterior access is required for arthroscopic treatment [25]. Abrupt signal changes of the articular cartilage can indicate a defect that is below the current MR morphological detection limit. Subchondral signal changes morphologically detected in the MRI can indicate cartilage lesions even if the cartilage defects themselves cannot be distinguished (▶ **Fig. 4**). Even slight bone marrow edema in MR imaging is sometimes the only indication of subtle cartilage damage in the ankle joint [25].

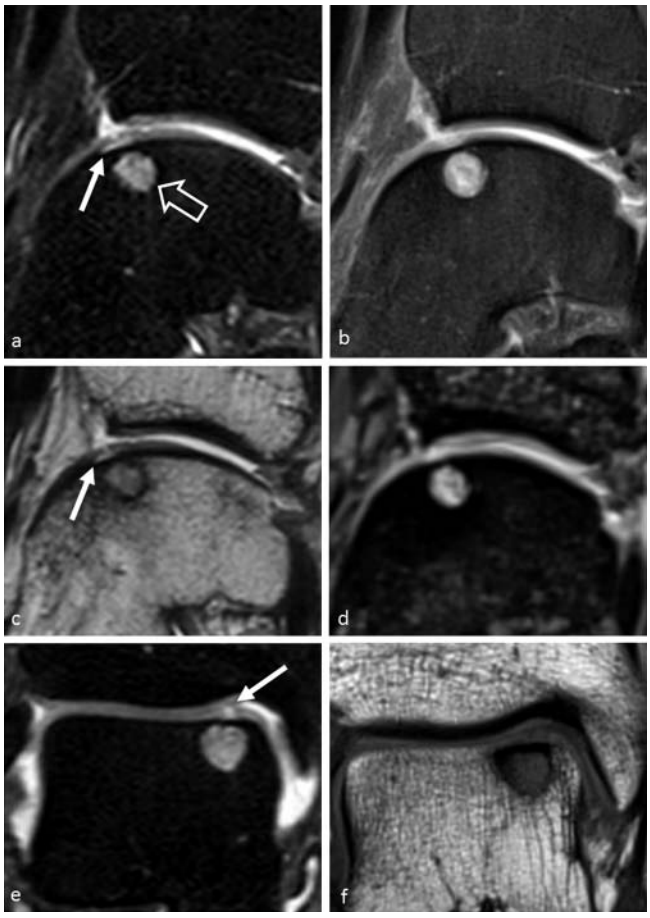

▶ **Fig. 2** 52-year-old-man with osteochondral lesion of the medial talar dome. **a** Sagittal proton density (PD) weighted fat suppressed 3 D SPACE sequence, **b** sagittal PD-weighted fat suppressed 2 D sequence, **c** sagittal PD-weighted 3 D SPACE sequence, **d** sagittal 3 D T2*-weighted MEDIC sequence, **e** coronal PD-weighted fat suppressed 3 D SPACE sequence, **f** coronal T1-weighting. With the help of high-resolution 3 D SPACE 3 Tesla sequences a thin line of fluid signal along the bone-cartilage interface (arrow) indicating that a larger cartilage delamination is present is visible. The cartilage delamination above the subchondral cyst (open arrow) is not visible at the 3 D MEDIC and the 2 D sequences.

▶ **Fig. 3** Sagittal T1-weighted 3 Tesla DRIVE sequence of the ankle without traction **a** and with axial traction (6 kg) of a healthy volunteer **b**. Axial traction leads to an increase in joint space width (arrow) and the visualization of the opposing cartilage surfaces **b**. Focal, full-thickness cartilage defect with delamination (arrow) at the medial talar dome depicted using 3 Tesla MRI and axial traction (6 kg) in a 33-year-old woman, **c** coronal T1-weighted DRIVE sequence, **d** coronal proton density (PD) weighted fat suppressed BLADE sequence and the same patient after treatment using osteochondral grafting (OATS, autologous osteochondral transplantation). **e** Coronal T1-weighted DRIVE and **f** coronal PD-weighted fat suppressed BLADE sequence. The osteochondral cylinder (open arrow) is well integrated and the cartilage overlay with minor irregularities of the cartilage surface is preserved.

Classification of osteochondral lesions

Osteochondral lesions of the ankle are the most common cause of cartilage damage. They have a singular age distribution between 15 and 35 years, and 63 % of the patients are male [27]. The osteochondral lesions occur predominantly in the talus with a ratio of occurrences in the tibial plateau to the talar dome of 1 to 20. Most osteochondral lesions are caused by trauma (94 % of lateral lesions and 62 % of medial OCL) [25, 28, 29]. The symptoms of OCL are unspecific ankle pain and swelling [25, 29], often associated with a limitation of dorsal extension. After acute ankle distortion, the incidence of OCL is estimated to be just under 7 % [25, 30]. When pain is persistent after ankle distortion, the incidence is markedly higher, as osteochondral lesions could be detected in 38 % of patients with persistent pain lasting over 7 months after ankle joint trauma [31]. However, an osteochondral lesion is often described as a random finding in the MRI without concomitant symptoms and is often asymptomatic [32]. Increasing lesion size and a high body mass index can be classified as prognostically unfavorable, whereas there are differing study results of OCL relating to the relationship between age and therapeutic success [32 – 34]. Osteochondral lesions differ in their localization on the talus into the anterior-superior-lateral OCL, which is mostly flat-configured and often caused by shear injuries, and posterior-superior-medial OCL, which is mostly deeper and crater-shaped, and is caused by repetitive trauma such as impact injuries [25] (▶ **Fig. 5a–b**).

There are several classifications of osteochondral lesions. In 1959 the first classification was introduced by Berndt & Harty based on projection radiography and histology of amputated limbs [35] (▶ **Fig. 5c**) It was found, however, that the 4 stages

▶ **Fig. 4** 38-year-old woman with tiny, deep, focal cartilage damage (arrow) at the medial talar dome. Sagittal **a** and coronal **b** proton density (PD) weighted fat suppressed 2 D sequence with 3 mm slice thickness and sagittal **c** and coronal **d** reconstructions of the CT-arthrogram (120 kV, 60 mAs, 2 mm slice thickness). When subchondral bone marrow edemas (open arrow) are encountered, the cartilage layer should be screened carefully for subtle cartilage damages.

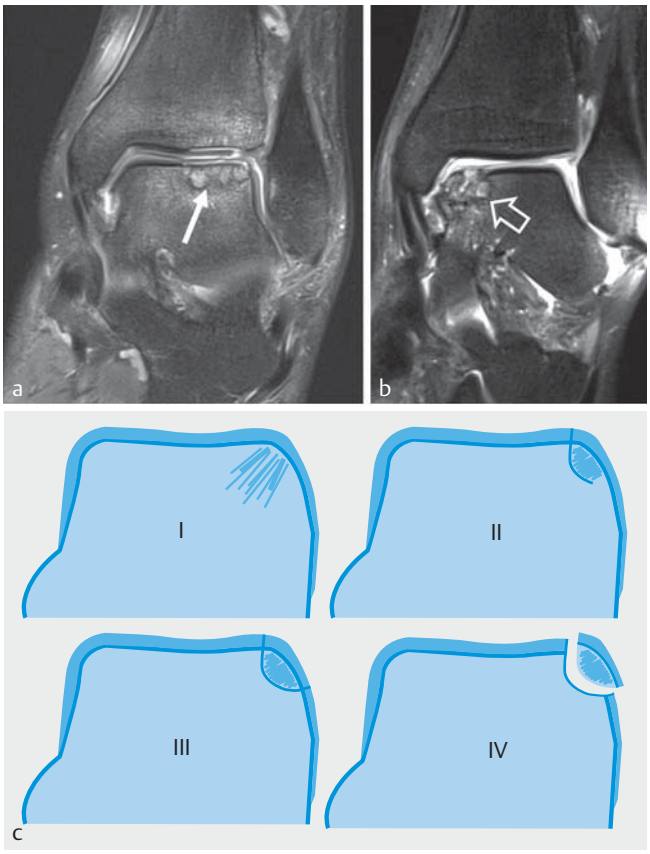

▶ **Fig. 5** Osteochondral lesions of the talar dome have two preferred locations: anterior-superior lateral **a** and posterior-superior medial **b** (coronal proton density weighted fat-suppressed sequence). The lateral osteochondral lesions of the talar dome are in most cases rather flat configurated (arrow), whereas the medial osteochondral lesions are in most cases deeper and crater-shaped (open arrow). **c** Classification scheme for osteochondral lesions as established by Berndt & Harty 1959 [35], modified from Griffith et al. 2012 [40].

proposed by Berndt & Harty were not accurate in the prediction of clinical outcome [25]. Based on arthroscopic findings, the International Cartilage Repair Society (ICRS) presented a graduated system, likewise with 4 stages [36]. By 2012, 10 different schemes had been described, including the widely used classifications according to Anderson [37] and Nelson & Dipaola [38, 39] (▶ **Table 2**) [40]. Important elements of these classification schemes are the presence of bone marrow edema, the integrity of the cartilage surface and the (remaining) connection or detachment of the osteochondral fragment. In 2012, Griffith et al. [40] proposed an MRI-based classification scheme which is shown in (▶ **Fig. 6**). This classification was developed in addition to standard 1.5 Tesla and 3 Tesla imaging using a high-resolution surface coil and sequences at 1.5 Tesla with a resolution of 0.3 to 0.4 mm within the slice [40]. However it can be applied to the standard 3 Tesla MRI protocol (▶ **Fig. 7**). Regardless of the classification scheme used, the crucial question for therapy is the clinical manifestation and whether an osteochondral lesion is stable or unstable. Among other criteria, the presence of a cartilage defect is an important instability criterion [32]. Therefore, in 2001, Bohndorf et al. suggested a two-stage scheme to help decide between conservative and surgical therapy [9]. In stage 1, the cartilage layer is intact, and there is contrast enhancement of the lesion in the subchondral bone. This stage of OCL is suitable for conservative treatment. On the other hand, in stage 2 of OCL surgical treatment is considered since there are cartilage defects or large cystic lesions greater than 5 mm in diameter, and the fragment shows little or no contrast medium absorption. Fluid may also be present around the non-dislocated fragment; there may be a partial fragment separation, or a free articular body [9].

General signs of fragment instability in native MRI are a signal-rich line around the OCL and an articular fracture of the cartilage layer with a T2w signal-rich line radiating into the lesion [25, 29] (▶ **Fig. 8**). Other signs of an unstable OCL are focal cartilage defects or defects in the subchondral bony end plate, the presence of subchondral cysts or an empty bony defect zone filled with fluid [25, 29]. However, mechanical stability assessment alone, based on MRI findings, has also been critically discussed [41], and one study of the knee demonstrated no relationship between the size and localization of an OCL and its stability [42]. The aforementioned signs of instability of an OCL apply to adults and adolescents with closed epiphyseal plates [25, 43]. In adolescents with open epiphyseal plates and children a signal-poor border (possibly as an expression of sclerosis) around the osteochondral lesion was described as a sign of instability in addition to the fluid

▶ **Table 2** Classification of osteochondral lesions according to Nelson & Dipaola, modified from [22].

stage	MRI finding
1	cartilage swelling and subchondral signal change
2	cartilage possibly fractured, subchondral fragment demarcation by hypointense line
3	cartilage fractured, fluid between fragment and adjoining bone
4	free articular body

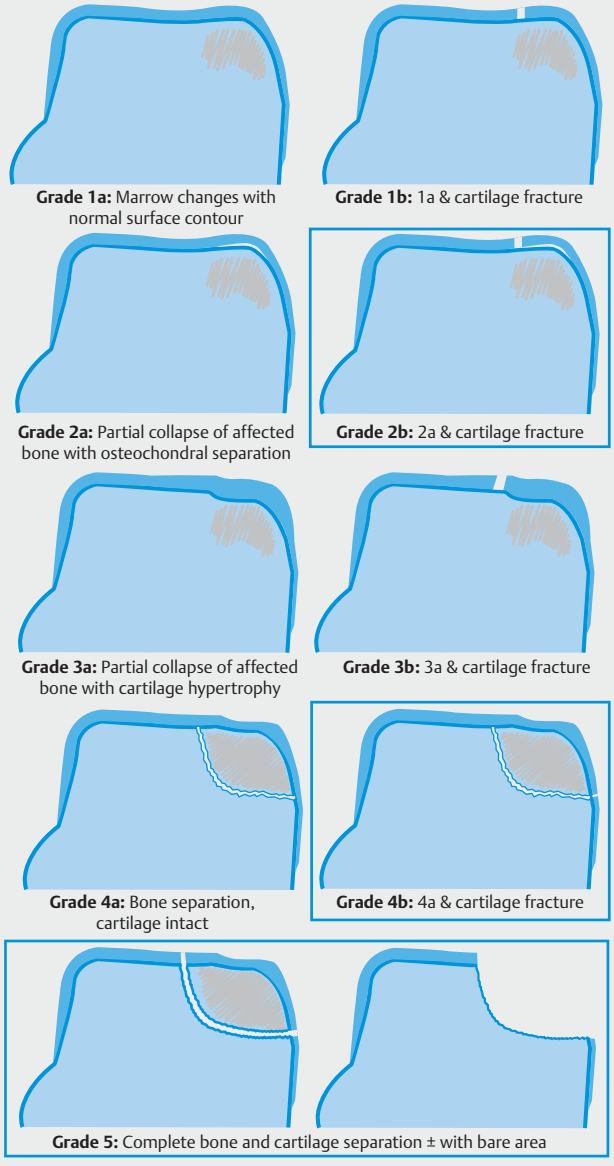

▶ **Fig. 6** Classification of osteochondral lesions according to Griffith et al. 2012 [40]. Instable lesions of variable severity are highlighted by a box.

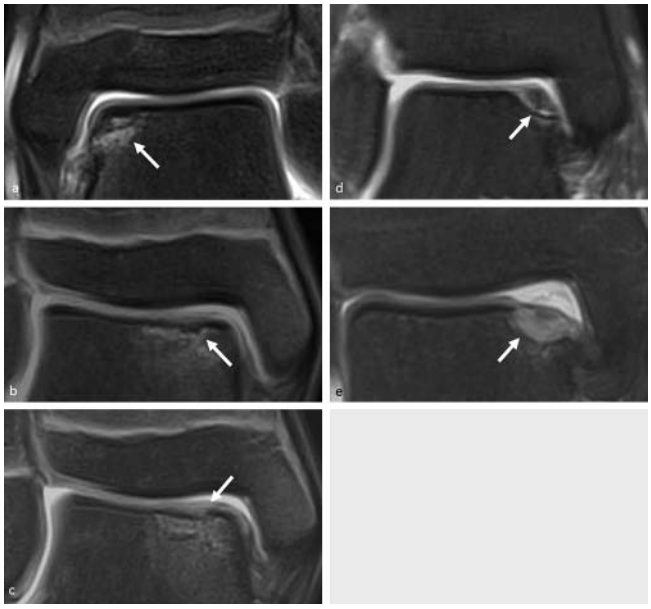

▶ **Fig. 7** MRI examples (**a–e**, coronal proton density weighted fat suppressed 2 D sequences) of osteochondral lesions, as classified according to Griffith et al. 2012 [40]. **a** Grade 1a: Subchondral bone marrow edema with normal surface contour. **b** Grade 2a: Partial collapse of affected subchondral bone with osteochondral separation. **c** Grade 3a: Partial collapse of affected bone with cartilage hypertrophy. **d** Grade 4a: Complete bony separation but intact cartilage surface. **e** Grade 5: Detachment with bare area.

border around the OCL fragment or (multiple) defects in the subchondral bony end plate [42, 43]. In contrast, cysts in association with an osteochondral lesion are not signs of instability in juvenile patients [25, 42], as shown in (▶ **Fig. 8e–f**).

Assessment of therapeutic results

Morphologically, the goal of therapy is the restoration of the cartilage surface and osteochondral integrity as well as achieving pain relief. This can be accomplished, on the one hand, by fibrocartilaginous repair tissue, e. g. after micro-fracturing or retrograde drilling of osteochondral lesions, or via transplant, using osteochondral autograft transfer (OATS) or the matrix-induced autologous chondrocyte transplantation (MACT) [27, 44]. In addition, micro-fracturing can be combined with matrix implantation as part of autologous matrix-induced chondrogenesis (AMIC) at the ankle joint; [19] provides a current overview of this. Knowledge of some basic features of the therapy of osteochondral lesions helps the radiologist in the classification of the findings. These can be summarized as follows without claiming to be complete, whereby, of course, the general individual clinical condition and the patient wishes must always be taken into account. As long as there is a stable situation without risk of a fragment breaking loose, conservative therapy can be carried out with a brief period of rest, or, depending on the degree of injury, immobilization or other relief for 6 – 8 weeks. This should be followed by a repeated MRI examination if the complaint persists [32]. If, despite rest and weight-bearing relief, no improvement is evident after 3 – 6 months, retrograde drilling to improve blood flow is a therapeu-

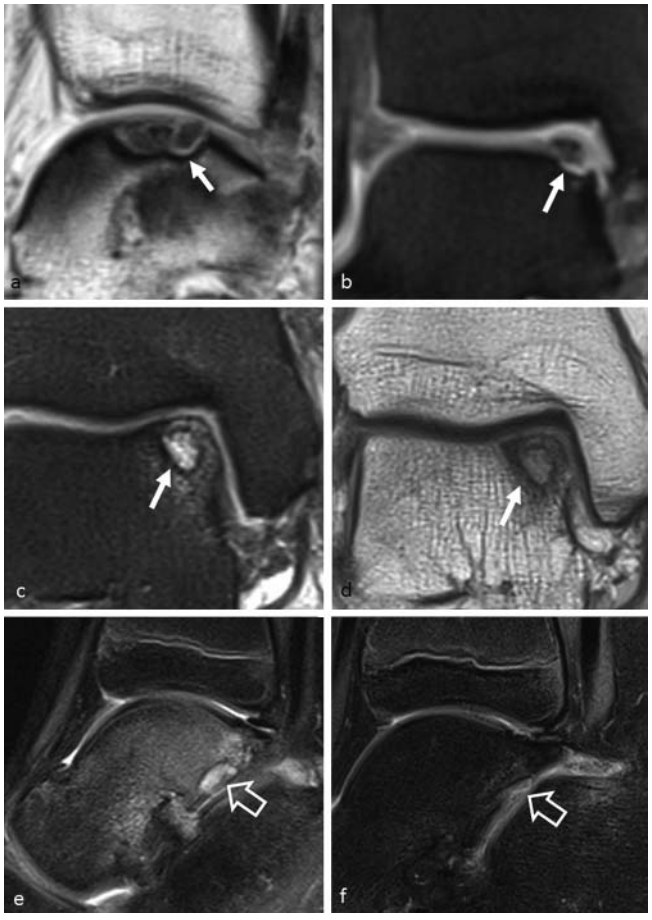

▶ **Fig. 8** Osteochondral lesions of the talus with signs of fragment instability. **a–b** 41-year-old woman with incidental finding of an osteochondral lesion, history of calcaneal fracture in childhood. High signal line (arrow) surrounding the lesion and medial disruption of the cartilage layer as signs of fragment instability; **a** sagittal proton density (PD) weighting, **b** coronal fat suppressed PD-weighting. **c–d** 64-year-old woman with load-dependent pain for 5 years that last about 5 days when occurring. No history of trauma; **c** coronal fat suppressed PD- and **d** coronal PD-weighting. The arrows point at the pronounced subchondral cyst as indication of fragment instability. **e-f** Illustration of healing of subtalar osteochondral lesion with cyst formation (open arrow in **e**) in a 10-year-old boy, who is pain free after 2 years **f**; **e–f** sagittal fat suppressed PD-weighting. Complete regression of the cyst and the bone marrow edema with constantly slight irregularity of the cartilage layer (open arrow in **f**). Cysts in association with osteochondral lesions are no signs of instability in the juvenile, in contrast to adults.

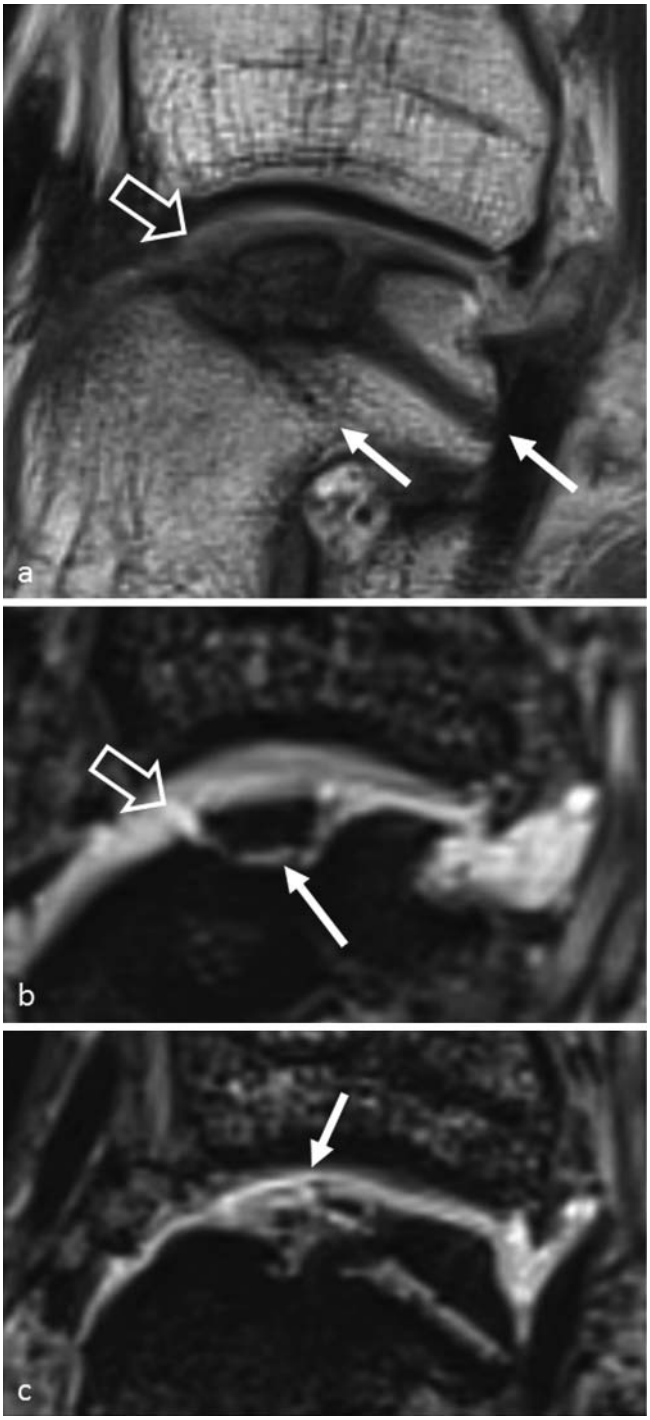

▶ **Fig. 9** 17-year-old woman with microfracture 4 years ago and retrograde fragment fixation 3 years ago, who still has pain during sports activities; **a** sagittal proton density (PD) weighted 2 D sequence with 2.5 mm slice thickness, **b–c** 3 D MEDIC sequence with isotropic voxel size of 0.6 mm^3. In the 2 D sequence the cartilage surface above the osteochondral lesion appears intact (open arrow in **a**), the arrows in **a** point at the retrograde drilling channels. The 3 D MEDIC sequence demonstrates signs of instability, which cannot be detected in the 2 D sequence, such as the high signal line surrounding the lesion, the articular fracture within the cartilage layer and the high signal line passing into the lesion (arrow in **c**). Therefore, a conservative treatment with periods of rest is not indicated.

tic option. In the case of an unstable situation in a child, reattachment of the osteochondral fragment with accompanying rejuvenation of the fragment bed by drilling is indicated. Additional subchondral spongiosaplasty is usually necessary for a spongiose defect. If the OCL bed is empty, cartilage and bone-regenerative therapy (OATS, MACT with spongiosaplasty or AMIC) may be carried out via drilling with microfracturing in addition to resection of the sclerotic zone [19, 32, 45].

The objectives of imaging after therapy are assessment of the technical success, such as the degree of defect replenishment, assessment of the morphology and peripheral integration of the

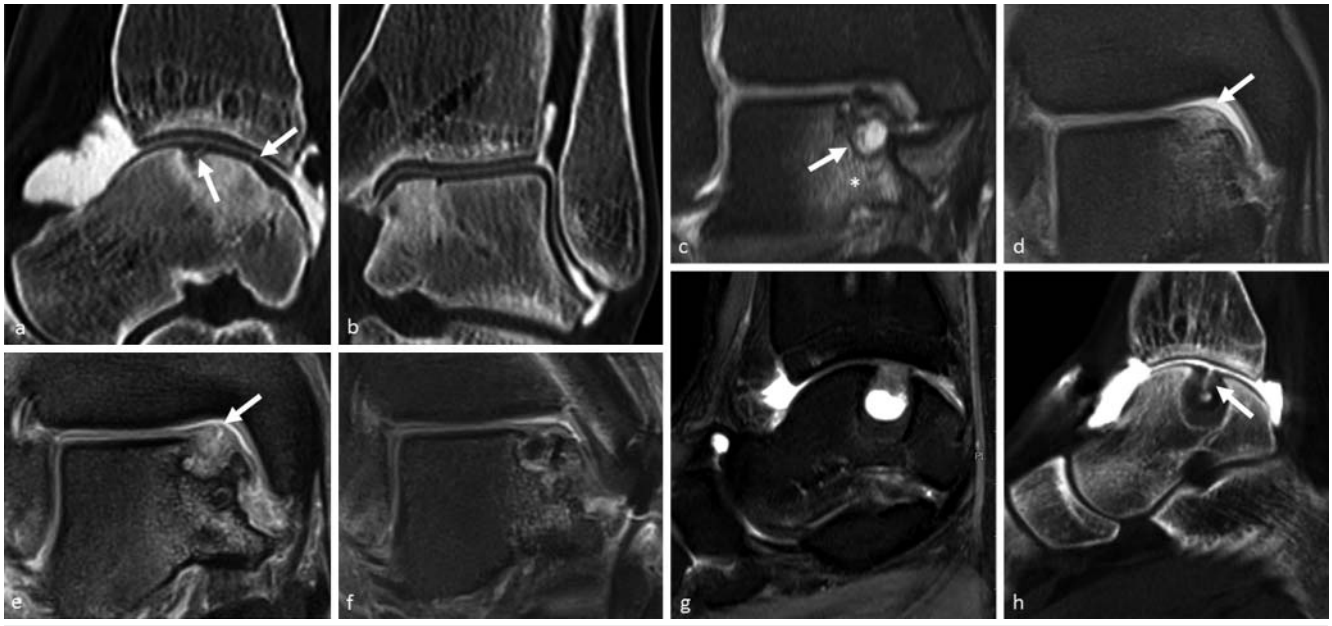

▶ **Fig. 10 a–b** CT-arthrograms (120 kV, 112 mAs) in sagittal **a** and coronal **b** reformation and 2 mm slice thickness in an 18-year-old woman after OATS (osteochondral autologous transplantation system). Despite the well-integrated bone-cartilage cylinder, the arrows in the sagittal reformations **a** point at subtle residual fissures at the border of the bone-cartilage cylinder to the normal cartilage layer. **c–f** Coronal proton density (PD)-weighted fat suppressed sequences in a 23-year-old woman with osteochondral lesion of the medial talar dome. **c** Initially there is bone marrow edema (asterisk) and a large subchondral cyst (arrow). Treatment was performed thereafter with microfracture. **d** 10 months after microfracture treatment good filling of the defect with reparative tissue and smooth appearance of the surface (arrow). **e** 20 months later there is a fissure within the repair cartilage (arrow). Because of increasing symptoms treatment consisted of implantation of a cylinder of cancellous bone and AMIC (autologous matrix-induced chondrogenesis) procedure using a medial malleolus osteotomy approach **f**. The patient is postoperatively satisfied with the result. Damage to the overlying cartilage, as present in this example, usually precludes a retrograde surgical repair approach. **g** Sagittal fat suppressed PD-weighting and **h** CT-arthrogram (120 kV, 112 mAs, 1 mm slice thickness) in a 20-year-old woman after refilling of an osteochondral lesion. The fissure within the bio matrix is only visible in the CT-arthrogram (arrow).

repair tissue. The newly developing fibrous cartilage after microfracturing does not have the biomechanical load-bearing capacity as hyaline articular cartilage, but it can maintain normal joint function over an extended period [44]. It is important to assess whether the articular surface is congruent, the cartilaginous tissue has the same thickness as the surrounding cartilage, the transition to the rest of the cartilage is continuous, and the surface of the repair tissue is smooth. Morphologically, this characterizes a successful course of therapy 1 – 2 years after microfracturing [44]. Assessment of the cartilage layer over time is important, since damage rules out a repeated retrograde repair of the osteochondral fragment [25]. In the course of successful therapy, the signal intensity of the repair tissue decreases in liquid-sensitive sequences and is similar to that of the rest of the cartilage; likewise the subchondral bone marrow edema disappears [44]. Signs of therapy failure can be the persistence of subchondral cysts and / or bone marrow edema, an irregular cartilage surface, incomplete defect filling as well as delamination of the cartilage layer, which usually occurs within the first 6 months after MACT or AMIC [44, 46] (▶ **Fig. 9 – 11**). Inadequate regeneration is more common after microfracturing compared to MACT or osteochondral transplants. If subchondral cysts occur after cartilage therapy, they should be measured with regard to their size, since filling with bone material may become necessary. Larger cyst formation and an interruption of the subchondral border lamella are associated with poorer treatment results [25]. In particular, inadequate healing of osteochondral cylinders predisposes formation of subchondral cysts by persistent fissural defects in the border zone, despite press-fit technique.

Functional biochemical cartilage imaging

Functional biochemical sequence techniques for cartilage imaging, such as dGEMRIC (delayed gadolinium enhanced MR imaging of cartilage) [47], can detect the change in cartilage matrix composition even before morphological changes are visible. The dGEMRIC technique shows a loss of glycosaminoglycans (GAG), which in turn is regarded as the initial event in arthrosis formation [48, 49] (▶ **Fig. 12**). T2 mapping can assess the water content and collagen fiber integrity of the articular cartilage [48, 50]. Increasing T2 relaxation times indicate early cartilage degeneration and destruction of the collagen fiber network. Both biochemical techniques can thus potentially display very early cartilage changes or can also be used to monitor biochemical changes (maturation) within the regenerated tissue after therapy (▶ **Fig. 12**). The extent to which these techniques or even certain dGEMRIC or T2 values correlate with clinical parameters is still unclear and is the subject of scientific investigations.

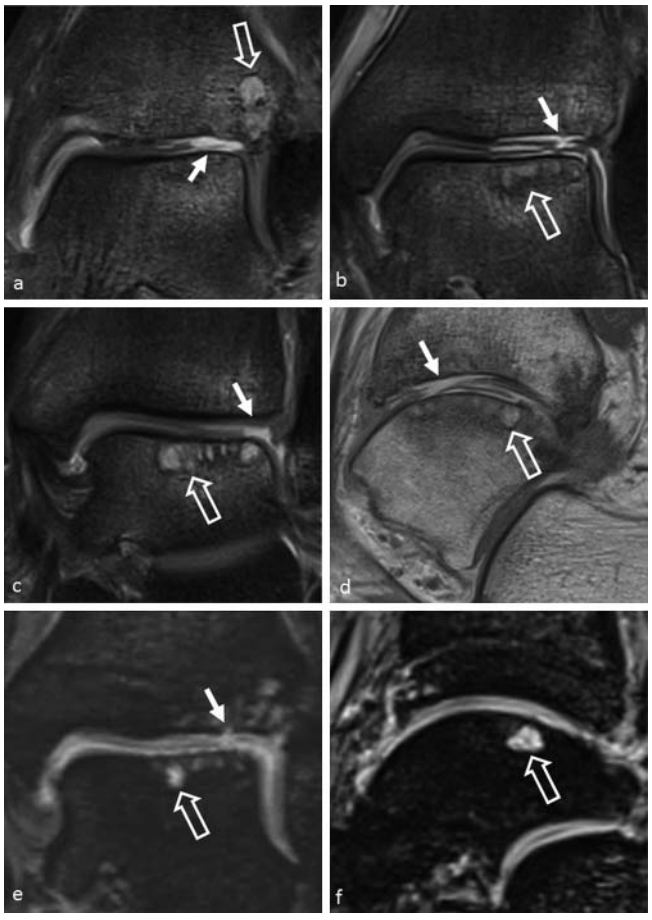

▶ **Fig. 11** 50-year-old man 2 years after microfracture therapy with chronic pain of his left ankle for 18 months that last the whole day because of kissing osteochondral lesions. **a–c** coronal proton density (PD) weighted fat suppressed sequences, **d** sagittal PD-weighting, 3 D T2*w MEDIC sequence in coronal **e** and sagittal reformation **f**. There are extensive delaminations of the tibial and talar cartilage on the lateral side (arrows in **a–d**) as well as subchondral cyst formation (open arrows), pronounced at the lateral talar dome and bone marrow edema. The coronal 3 D sequence also shows the focal disruption of the subchondral bone-cartilage interface (arrow). Because of the extensive findings we recommend arthrodesis of the ankle joint.

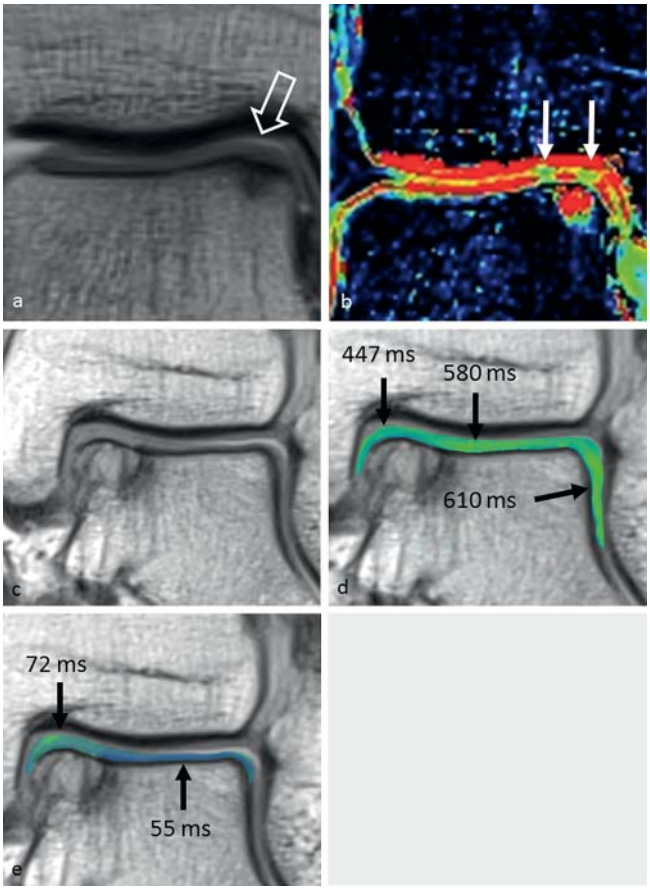

▶ **Fig. 12** **a, b** 31-year-old man with osteochondral lesion of the medial talar dome; **a** coronal proton density (PD) weighting, **b** dGEMRIC parameter map. While the cartilage layer is morphologically uneventful, there are two areas with decreased T1 values (arrows) in the dGEMRIC parameter map that point at a focal loss of glycosaminoglycans. **c–e** 61-year-old man with osteochondral lesion of the medial talar dome; **c** coronal PD-weighting, **d** dGEMRIC parameter map superimposed on the PD-weighting, **e** T2-mapping parameter map superimposed on the PD-weighting. There are decreased T1 values within the cartilage overlay of the osteochondral lesion **d**, which argue for a loss of glycosaminoglycans within the cartilage overlay. In addition, there are also increased T2 values **e**, which argue for an increase in water content and degeneration of the collagen fiber network.

Summary

Current native MRI allows high-resolution imaging of the thin articular cartilage of the upper ankle and, in comparison to arthroscopy, also demonstrates subchondral pathologies. Advances in MRI, especially through the development of isotropic 3 D sequences with high signal-to-noise ratio or contrast-to-noise ratio for imaging the ankle cartilage as well as the axial traction technique frequently make adequate assessment of the ankle cartilage possible. Compared to standard 2 D sequences, imaging of the ankle using isotropic 3 D sequences also results in fewer partial volume effects. If MRI is contraindicated, CT arthrography can be also employed to further diagnose ambiguous MRI findings. It can also very sensitively detect cartilage damage, including fissural defects. Imaging of osteochondral lesions should be performed in several spatial planes for the complete assessment of cartilage integrity, articular surface depression, subchondral bone and fragment stability. When classifying an OCL it is important to use the same points of reference as the treating orthopedic colleague and to agree on the use of a classification, e. g. simple classification into 4 stages according to Nelson & Dipaola with supplementary finding measurement and description.

Conflict of Interest

The authors declare that they have no conflict of interest.

References

[1] Rodgers MM. Dynamic foot biomechanics. J Orthop Sports Phys Ther 1995; 21: 306 – 316

[2] Egloff C, Hügle T, Valderrabano V. Biomechanics and pathomechanisms of osteoarthritis. Swiss Med Wkly 2012; 142: w13583

[3] Stufkens SA, Knupp M, Horisberger M et al. Cartilage lesions and the development of osteoarthritis after internal fixation of ankle fractures: a prospective study. J Bone Joint Surg Am 2010; 92: 279 – 286

[4] Verhagen RA, Maas M, Dijkgraaf MG et al. Prospective study on diagnostic strategies in osteochondral lesions of the talus. Is MRI superior to helical CT? J Bone Joint Surg Br 2005; 87: 41 – 46

[5] O'Loughlin PF, Heyworth BE, Kennedy JG. Current concepts in the diagnosis and treatment of osteochondral lesions of the ankle. Am J Sports Med 2010; 38: 392 – 404

[6] Grambart ST. Arthroscopic management of osteochondral lesions of the talus. Clin Podiatr Med Surg 2016; 33: 521 – 530

[7] Schmid MR, Pfirrmann CW, Hodler J et al. Cartilage lesions in the ankle joint: comparison of MR arthrography and CT arthrography. Skeletal Radiol 2003; 32: 259 – 265

[8] Shepherd DE, Seedhom BB. Thickness of human articular cartilage in joints of the lower limb. Ann Rheum Dis 1999; 58: 27 – 34

[9] Bohndorf K, Imhof H, Schibany N. Bildgebende Diagnostik akuter und chronischer osteochondraler Läsionen am Talus. Orthopäde 2001; 30: 12 – 19

[10] Barr C, Bauer JS, Malfair D et al. MR imaging of the ankle at 3 Tesla and 1.5 Tesla: protocol optimization and application to cartilage, ligament and tendon pathology in cadaver specimens. Eur Radiol 2007; 17: 1518 – 1528

[11] Mengiardi B, Pfirrmann CW, Schöttle PB et al. Magic angle effect in MR imaging of ankle tendons: influence of foot positioning on prevalence and site in asymptomatic subjects and cadaveric tendons. Eur Radiol 2006; 16: 2197 – 2206

[12] Nierhoff CE, Ludwig K. Magnetresonanztomographie des Sprunggelenkes. Radiologe 2006; 46: 1005 – 1020

[13] AG Muskoloskelettale Diagnostik der Deutschen Röntgengesellschaft. Von der AG Muskuloskelettale Diagnostik der Deutschen Röntgengesellschaft empfohlene Protokolle für MRT-Untersuchungen der Gelenke und Wirbelsäule. Fortschr Röntgenstr 2006; 178: 128 – 130

[14] Notohamiprodjo M, Kuschel B, Horng A et al. 3D-MRI of the ankle with optimized 3D-SPACE. Invest Radiol 2012; 47: 231 – 239

[15] Stevens KJ, Busse RF, Han E et al. Ankle: isotropic MR imaging with 3D-FSE-cube – initial experience in healthy volunteers. Radiology 2008; 249: 1026 – 1033

[16] Yi J, Cha JG, Lee YK et al. MRI of the anterior talofibular ligament, talar cartilage and os subfibulare: Comparison of isotropic resolution 3D and conventional 2D T2-weighted fast spin-echo sequences at 3.0 T. Skeletal Radiol 2016; 45: 899 – 908

[17] Jungmann PM, Baum T, Schaeffeler C et al. 3.0T MR imaging of the ankle: Axial traction for morphological cartilage evaluation, quantitative T2 mapping and cartilage diffusion imaging-A preliminary study. Eur J Radiol 2015; 84: 1546 – 1554

[18] Woertler K, Rummeny EJ, Settles M. A fast high-resolution multisliceT1-weighted turbo spin-echo (TSE) sequence with a DRIVen equilibrium (DRIVE) pulse for native arthrographic contrast. Am J Roentgenol 2005; 185: 1468 – 1470

[19] Aurich M, Albrecht D, Angele P et al. Treatment of Osteochondral Lesions in the Ankle: A Guideline from the Group "Clinical Tissue Regeneration" of the German Society of Orthopaedics and Traumatology (DGOU). Z Orthop Unfall 2017; 155: 92 – 99

[20] Kirschke JS, Braun S, Baum T et al. Diagnostic Value of CT arthrography for evaluation of osteochondral lesions at the ankle. Biomed Res Int 2016; 2016: 3594253

[21] Cerezal L, Llopis E, Canga A et al. MR arthrography of the ankle: indications and technique. Radiol Clin North Am 2008; 46: 973 – 994

[22] Waldt S, Eiber M, Wörtler K. Gelenkknorpel. In: Messverfahren und Klassifikationen in der muskuloskelettalen Radiologie. Stuttgart-New York: Thieme; 2011: 174 – 179

[23] Masala S, Fiori R, Bartolucci DA et al. Diagnostic and therapeutic joint injections. Semin Intervent Radiol 2010; 27: 160 – 171

[24] Steinbach LS, Palmer WE, Schweitzer ME. Special focus session. MR arthrography. Radiographics 2002; 22: 1223 – 1246

[25] Forney M, Subhas N, Donley B et al. MR imaging of the articular cartilage of the knee and ankle. Magn Reson Imaging Clin N Am 2011; 19: 379 – 405

[26] Cuttica DJ, Smith WB, Hyer CF et al. Osteochondral lesions of the talus: predictors of clinical outcome. Foot Ankle Int 2011; 32: 1045 – 1051

[27] Zengerink M, Struijs PA, Tol JL et al. Treatment of osteochondral lesions of the talus: a systematic review. Knee Surg Sports Traumatol Arthrosc 2010; 18: 238 – 246

[28] Parisien JS. Arthroscopic treatment of osteochondral lesions of the talus. Am J Sports Med 1986; 14: 211 – 217

[29] Winalski CS, Alparslan L. Imaging of articular cartilage injuries of the lower extremity. Semin Musculoskelet Radiol 2008; 12: 283 – 301

[30] Bosien WR, Staples OS, Russell SW. Residual disability following acute ankle sprains. J Bone Joint Surg Am 1955; 37-A: 1237 – 1243

[31] Takao M, Uchio Y, Naito K et al. Arthroscopic assessment for intra-articular disorders in residual ankle disability after sprain. Am J Sports Med 2005; 33: 686 – 692

[32] Von Stillfried E, Weber MA. Aseptische Osteonekrosen bei Kindern und Jugendlichen. Orthopäde 2014; 43: 750 – 757

[33] Becher C, Driessen A, Thermann H. Microfracture technique for the treatment of articular cartilage lesions of the talus. Orthopäde 2008; 37: 196 – 203

[34] Kuni B, Schmitt H, Chloridis D et al. Clinical and MRI results after microfracture of osteochondral lesions of the talus. Arch Orthop Trauma Surg 2012; 132: 1765 – 1771

[35] Berndt AL, Harty M. Transchondral fractures (osteochondritis dissecans) of the talus. J Bone Joint Surg 1959; 41: 988 – 1020

[36] International Cartilage Repair Society (ICRS). ICRS Cartilage Injury Evaluation Package 2000. Im Internet: http://cartilage.org/content/uploads/2014/10/ICRS_evaluation1-1.pdf; Stand: 04.10.16

[37] Anderson IF, Crichton KJ, Grattan-Smith T et al. Osteochondral fractures of the dome of the talus. J Bone Joint Surg Am 1989; 71: 1143 – 1152

[38] Dipaola JD, Nelson DW, Colville MR. Characterizing osteochondral lesions by magnetic resonance imaging. Arthroscopy 1991; 7: 101 – 104

[39] Nelson DW, Dipaola J, Colville M et al. Osteochondritis dissecans of the talus and knee: prospective comparison of MR and arthroscopic classifications. J Comput Assist Tomogr 1990; 14: 804 – 808

[40] Griffith JF, Lau DT, Yeung DK et al. High-resolution MR imaging of talar osteochondral lesions with new classification. Skeletal Radiol 2012; 41: 387 – 399

[41] Elias I, Jung JW, Raikin SM et al. Osteochondral lesions of the talus: change in MRI findings over time in talar lesions without operative intervention and implications for staging systems. Foot Ankle Int 2006; 27: 157 – 166

[42] Kijowski R, Blankenbaker DG, Shinki K et al. Juvenile versus adult osteochondritis dissecans of the knee: appropriate MR imaging criteria for nstability. Radiology 2008; 248: 571 – 578

[43] De Smet AA, Ilahi OA, Graf BK. Reassessment of the MR criteria for stability of osteochondritis dissecans in the knee and ankle. Skeletal Radiol 1996; 25: 159 – 163

[44] Choi YS, Potter HG, Chun TJ. MR imaging of cartilage repair in the knee and ankle. Radiographics 2008; 28: 1043 – 1059

[45] Murawski CD, Kennedy JG. Operative treatment of osteochondral lesions of the talus. J Bone Joint Surg Am 2013; 95: 1045 – 1054

[46] Cuttica DJ, Shockley JA, Hyer CF et al. Correlation of MRI edema and clinical outcomes following microfracture of osteochondral lesions of the talus. Foot Ankle Spec 2011; 4: 274 – 279

[47] Burstein D, Velyvis J, Scott KT et al. Protocol issues for delayed Gd (DTPA)(2^-)-enhanced MRI (dGEMRIC) for clinical evaluation of articular cartilage. Magn Reson Med 2001; 45: 36 – 41

[48] Rehnitz C, Weber MA. Morphologische und funktionelle Knorpeldiagnostik. Orthopäde 2015; 44: 317 – 336

[49] Zilkens C, Jäger M, Bittersohl B et al. Delayed Gadolinium Enhanced MRI of Cartilage (dGEMRIC) – Molekulare MRT-Bildgebung des Hüftgelenkknorpels. Orthopäde 2009; 38: 591 – 599

[50] Liess C, Lüsse S, Karger N et al. Detection of changes in cartilage water content using MRI T2-mapping in vivo. Osteoarthritis Cartilage 2002; 10: 907 – 913